POLSKIE TOWARZYSTWO AKUSTYCZNE

KOMITET AKUSTYKI PAN

INSTYTUT FIZYKI POLITECHNIKI ŚLĄSKIEJ

57. Otwarte Seminarium z Akustyki

Element directivity influence in the synthetic focusing algorithm for ultrasound imaging

Yuriy TASINKEVYCH, Andrzej NOWICKI, Ihor TROTS
Institute of Fundamental Technological Research, Polish Academy of Sciences
Pawinskiego 5b, 02-106 Warsaw
E-mail: yurijtas@ippt.gov.pl

Abstract

The paper describes the modified synthetic focusing (SF) algorithm for ultrasound imaging. Synthetic focusing method being a particular case of the synthetic aperture (SA) technique is an alternate to a conventional phased array. At each time one array element transmits an ultrasound pulse and all the elements receive the echo signals. The modification discussed here concerns a directivity property of array element which becomes significant as the element width becomes comparable to the wavelength corresponding to the nominal frequency of transmit signal. The angular dependence of the radiation efficiency of array element is approximated by a far-field radiation pattern of a single narrow strip transducer excited by a time harmonic uniform pressure distribution over its width. The corresponding function is calculated at the nominal frequency of excitation signal and is incorporated into the conventional SF imaging algorithm. The comparison of the modified and conventional SF algorithms by means of numerical experiments performed with the help of FIELD II simulation program for MATLAB environment reveals significant improvement of the image quality in the region close to the aperture as well as increase in the imaging depth.

1. INTRODUCTION

Ultrasound imaging has become one of the primary techniques for medical imaging mainly due to its accessibility, non-ionizing radiation, and real-time display. High resolution ultrasound images can be obtained by using array transducers and advanced beam-forming techniques. However, while array transducers make it possible to obtain high resolution images, manufacturing array transducer elements for applications at frequencies greater than 30 MHz is expensive and hard to achieve. Therefore, single-element transducers are used commonly in high frequency ultrasonic imaging. As a result, due to the fixed focal length of single element transducers, the lateral resolution outside the focal region become poor. Synthetic aperture imaging may offer a solution to this problem. Synthetic aperture imaging techniques were initially implemented in remote sensing/imaging by radar and were then used in sonar imaging. Synthetic aperture imaging technique also known as synthetic aperture focusing technique (SAFT) has been applied to ultrasound imaging [1]. Synthetic aperture is a post-processing reconstruction technique which utilizes a single element transducer to synthesize the effect of a larger aperture. Several methods were proposed to form a synthetic aperture for ultrasonic imaging. In SAFT imaging, at each time only a single array element transmits a pulse and receives the echo signal [2, 3]. Multi-element synthetic aperture focusing (M-SAF) is an alternate to SAFT [4]. A group of elements transmit and receive signals simultaneously, and transmit beam is unfocused to emulate a single element response. The acoustic power and the signal-to-noise ratio are increased as compared to SAFT where a single element is used. Synthetic focusing method (SF) [5] is an alternate to a conventional phased array. At each time a single array element transmits an ultrasound pulse and all elements receive the echo signals. The advantage of this approach is that a full dynamic focusing can be applied to both transmit and receive modes, giving the highest imaging quality. The synthetic transmit aperture (STA) [6, 7] is done by splitting transmit aperture into several sub-apertures. At each time one sub-aperture transmits an ultrasound pulse and all the elements receive the echo signals. In all this methods it is assumed that the transmit and receive elements are the point-like sources and the dynamical focusing is realized by finding the geometric distance from the transmitting element to the imaging point and back to the receiving element. But when the element size is comparable to the wavelength the influence of the element direcivity on the wave field generation and reception become significant and if ignored might be a source of errors and noise artefacts in the resulting image. In this paper we endeavor to modify the SF algorithm in order to take into account the single element directivity to improve the quality of the resulting image. For this purpose the array element is modeled as a narrow strip transducer with a time harmonic uniform pressure distribution over its width for the far-field radiation pattern calculation. An analytical expression for the corresponding directivity function is available in literature [8]. The far-field assumption is shown to be acceptable in the considered cases of the transducer dimension to wavelength ratios. The paper is organized as follows. In the next section the brief discussion of synthetic focusing algorithm is given. In Sec. 3 the modified algorithm is discussed for the SF case. The model of a narrow strip transducer is briefly discussed for the purpose of the far-field radiation pattern calculation, which approximates the directivity property of transmit-receive array element. And finally in Sec. 4 some results of numerical experiments performed by means of the FIELD II simulation program [9] for MATLAB environment are given.

2. SYNTHETIC FOCUSING ALGORITHM

As an alternate to the conventional phased array imaging technique a synthetic focusing method [5] can be used. It provides for the full dynamic focusing both in transmit and receive modes yielding the highest imaging quality. In this method, a full aperture is synthesized by using multiple firings. On each firing, a single element acts as a transmitter and all elements as the receivers. For an N-element array, $N\times N$ independent recordings are required to synthesize an N-element phased array in both transmit and receive modes. Conceptually, an SF system has all the characteristics of a conventional phased array. The depth of field is extended without any reduction in frame rate. The focusing is performed by finding the geometric distance from the transmitting element to the imaging point and back to the receiving element. The structure of the synthetic aperture and geometric relation between the transmit and receive element combination is shown in Fig. 1.

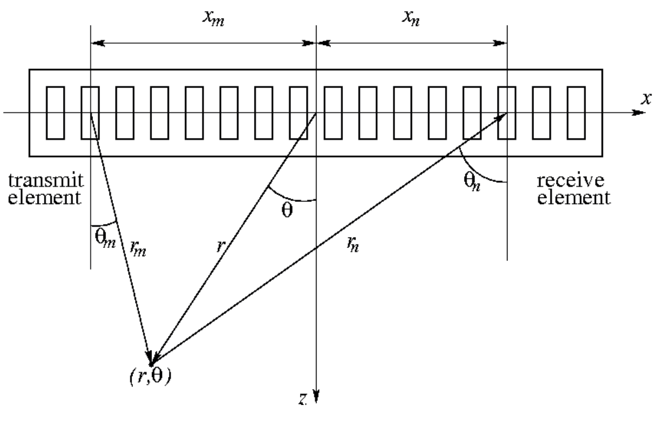

Fig. 1. Geometric relation between the transmit and receive element combination and the focal point

When a short pulse is transmitted by the element m and the echo signal is received by the element n, as shown in Fig. 1, the round-trip delay is

$$\tau_{m,n}=\tau_m+\tau_n, \qquad (1)$$

where (m, n) is the transmit-receive element combination, $1 \le m, n \le N$. The corresponding delays for m'th and n'th element relative to the imaging point (r,θ) are

$$\tau_i=\frac{1}{c}\left(r-\sqrt{r^2+x_i^2-2x_i r\sin(\theta)}\right),\ i=m,n\ , \qquad (2)$$

where x_m, x_n are the positions of the m'th and n'th elements, respectively, and r, θ are the polar coordinates of the imaging point (r,θ) with respect to the origin placed in the center of the transducer's aperture. In the case of the N-element array for each point in the image, the A-scan signal can be expressed as follows

$$A(r,\theta)=\sum_{m=1}^{N}\sum_{n=1}^{N} y_{m,n}\left(\frac{2r}{c}-\tau_{m,n}\right), \qquad (3)$$

where $y_{m,n}(t)$ is the echo signal and $\tau_{m,n}$ is the round-trip delay defined in (1) for the (m, n) transmit-receive element combination. The first and the second summations correspond to the transmit and receive beam-forming, respectively.

3. MODIFIED SF ALGORITHM

In the described above SF algorithm for each point in the resulting image every combination of transmit-receive pairs contributes according to the round-trip propagation time only. The angular dependence is not taken into account in the applied point-like source model. But when the width of the array element is comparable to the wavelength corresponding to the nominal frequency of the emitted signal, the point-like source model becomes inaccurate. The element directivity influences the partial contribution to the resulting signal $A(r,\theta)$ in (3) depending on the mutual position of the imaging point and transmit- receive pair, determined by the angles θ_m, θ_n (see Fig. 1). In this section we develop a modified SF imaging algorithm which accounts for the element directivity function and its influence on $A(r,\theta)$. The underlying idea can be illustrated on the following example shown in Fig. 2. Let us assume the case when the same element transmits and receives signal. Two scatterers located at the points with polar coordinates (r_i,θ_i), i=1,2 such that $r_{1m}=r_{2m}$ would contribute to the corresponding echo signal $y_{m,m}(t)$ simultaneously, since the round-trip propagation time $2r_{im}/c$, i=1,2 is the same. Apparently, the contribution from the scatterer at the point (r_1,θ_1) would be dominant, since the observation angle θ_{1m} coincides with the direction of maximum radiation for the m-th element, whereas its transmit-receive efficiency at the angle θ_{2m} is much smaller for the case of the scatterer at the point (r_2,θ_2). Thereby, evaluating the value of $A(r_2,\theta_2)$ from (3), the partial contribution of the echo $y_{m,m}(t)$ in addition to the correct signal from the obstacle located at (r_2,θ_2) (being small due to the large observation angle θ_{2m}), would also introduce the erroneous signal from the scatterer located at (r_1,θ_1). The latter signal is larger due to the small observation angle θ_{1m}. The larger observation angles appear in the imaging region close to the array aperture. Therefore, the most appreciable deviation from the point-like source model of the array element will occur there. A solution to the problem is proposed which accounts for the observation angle in accordance with the array element directivity function. Assume that the dependence of the transmit-receive efficiency of a single array element versus the observation angle is known and is denoted by $f(\theta_m)$, where θ_m is measured from the line parallel to z-axis and passing through the m-th element center. Thus, in order to suppress the erroneous influence from the scatterer located at (r_1,θ_1) on the value of the resulting signal $A(r_2,\theta_2)$, the partial contribution of the echo $y_{m,m}(t)$ is weighted by the corresponding value of $f(\theta_{2m})$. This corresponds to the superposed signal correction in accordance with respective contributions of individual scatterers located at the points (r_1,θ_1) and (r_2,θ_2).

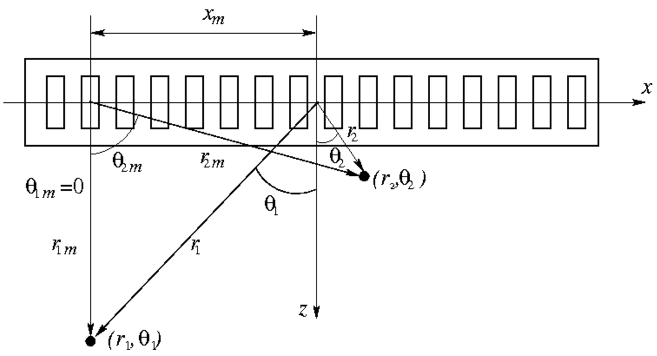

Fig. 2. Influence of the scatterer located at the point (r_1,θ_1) on the value of resulting signal $A(r_2,\theta_2)$ for imaging point (r_2,θ_2)

The above considerations lead to the following modification of the SF imaging algorithm

$$A(r,\theta)=\sum_{m=1}^{N}\sum_{n=1}^{N} f(\theta_m) f(\theta_n)\, y_{m,n}\left(\frac{2r}{c}-\tau_{m,n}\right), \tag{4}$$

where $\theta_i(r,\theta)$, $i=m,n$ are the corresponding observation angles for the transmit-receive pair. Note, that the angles depend on the spatial location of the imaging point (r,θ). The directivity function $f(\theta)$ can be calculated in the far-field approximation for a single element of the array transducer in analogous manner as in [8]

$$f(\theta)=\frac{\sin(\pi\, d/\lambda \sin\theta)}{\pi\, d/\lambda \sin\theta}\cos\theta, \tag{5}$$

where d is the element width, and λ is the wavelength. The above result applies to a narrow strip transducer with a time harmonic uniform pressure distribution along its width. It is obtained by means of the Rayleigh-Sommerfeld formula in the far-field region. The result is in a good agreement with experimental studies as shown by the authors in the cited work. For simplicity, we apply (5) in the numerical results presented in the next section. It should be noted, that we use the angular response $f(\theta)$ in (4) evaluated from (5) for some fixed value of λ which corresponds to the nominal frequency of the transmitted signal both in transmit and receive modes. The far-field approximation is admissible for the case of SF algorithm discussed here. For the typical examples considered in the next section, the ratio d/λ=1.125 is assumed. The far-field limit $r_{min} \approx 2d^2/\lambda$ [10] is 2.5λ, which requirement is met in the considered numerical experiments.

4. NUMERICAL RESULTS AND DISCUSSION

The numerical results presented in this section were performed by means of the FIELD II simulation program [9] for MATLAB environment. A 48-element linear transducer array excited by one sine cycle burst pulse at a nominal frequency of 5 MHz is assumed. The element pitch is 1.5λ and the inter-element spacing is 0.25 of the pitch, where λ corresponds to the nominal frequency of the burst pulse. The SF algorithm is employed which means that each time only a single element transmits the probing signal and all the elements receive the echoes. The transmit and receive elements combinations give a total of 48×48 possible RF A-lines. All these A-lines echo signals are sampled independently at a frequency of 50 MHz and stored in RAM. In Fig. 3 the results of simulation of a wire phantom are shown. Thin wires are spaced equidistantly with internals of 6λ in the lateral and axial directions. Fig. 3a corresponds to the modified SF algorithm (4) with the angular directivity function calculated according to (5), whereas in Fig. 3b the results corresponding to the conventional SF algorithm (3) are shown for comparison.

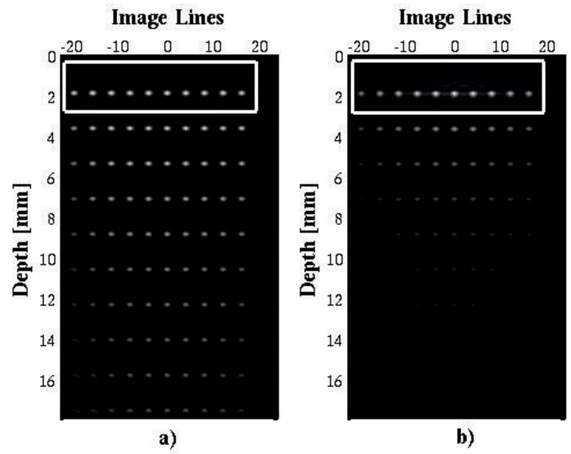

Fig. 3. Thin wire phantom simulation using modified a) and conventional b) SF algorithm. A 48-element linear array with element pitch of 1.5λ and inter-element spacing of 0.25 of the pitch is excited by one sine cycle burst pulse at a nominal frequency of 5 MHz; absolute values.

It is observable that the artefacts around the scatterers near the transducer aperture that are appreciable in the case of the conventional SF algorithm, are substantially suppressed in the case of the modified algorithm. This is illustrated in details in Fig. 4 where the selected region of the phantom is shown. Moreover, the scatterers located deeper are hardly noticeable in Fig. 3b, whereas in the case of the modified SF algorithm they are plainly distinguishable. The above example confirms that the simple modification of the SF algorithm, discussed in sec. 3, yields considerable improvement of the imaging quality in the region close to the transducer aperture and increase in the visualization depth at the same time.

4. CONCLUSION

In this work the modified synthetic focusing algorithm for ultrasound imaging is presented and discussed. The modification is based on the array element angular directivity incorporation into the conventional method. It is shown the the far-field radiation pattern of a narrow strip transducer calculated for the case of a time harmonic uniform pressure distribution over its width can serve as a good approximation for the above directivity function.

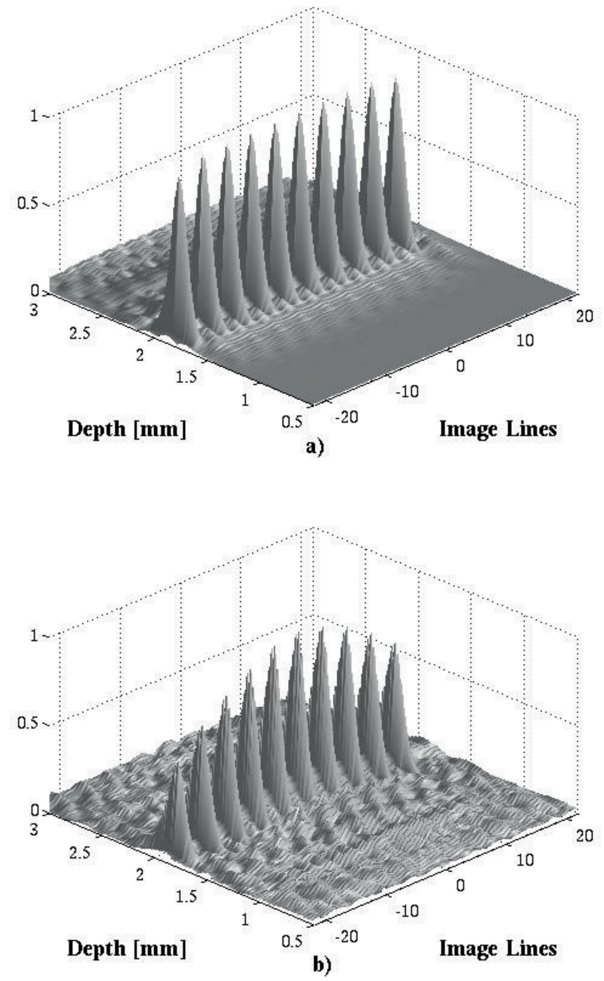

Fig. 4. Part of the phantom selected in Fig. 3 for the case of modified a) and conventional b) SF algorithm;absolute values.

The numerical results obtained by means of the FIELD II simulation program for MATLAB environment has shown distinguishable improvement of imaging quality in the phantom region near the transducer aperture. The artefacts in the form of hazy blurring, observable in the case of conventional SF algorithm are substantially suppressed in the case of the modified SF algorithm. Besides, the imaging depth is also increased, which is the valuable virtue of the developed method. It seems to be perspective to work further on the presented approach. Namely, the experimental results would be a good verification of the method. One of the possible continuations of the research is an application of the concept of directivity function calculated for different spectral components of the transmit-receive signal separately instead of using the far-field radiation pattern calculated for the fixed wavelength. Also it seems to be perspective to implement a similar modification into the synthetic transform aperture (STA) method for the cases of not large transmit apertures. Another possibility is to use a model of a finite system of narrow strips instead of a single strip transducer in order to calculate the far-field radiation pattern. This would account for the influence of interaction of the array elements and require the solution of the boundary value problem for strips.

ACKNOWLEDGMENTS

This work was supported by the Polish Ministry of Science and Higher Education (Grant NN518382137).

REFERENCES

[1] J. A. Jensen, S. I. Nikolov, K. L. Gammelmark, M. H. Pedersen, *Synthetic aperture ultrasound imaging*, Ultrasonics 44, Suppl., 2006, e5–e15.

[2] M. O'Donnell, L. J. Thomas, *Efficient synthetic aperture imaging from a circular apertur with possible application to catheter-based imaging*, IEEE Trans. Ultrason. Ferroelec. Freq. Contr., 39(3), 1992, 366–380.

[3] R. N. Thomson, *Transverse and longitudinal resolution of the synthetic aperture focusing technique,* Ultrasonics 22 (1), 1984, 9–15.

[4] D. H. Johnson, D. E. Dudgeon, Array Signal Processing: Concepts and Techniques. Prentice- Hall, 1993.

[5] G. E. Trahey, L. F. Nock, *Synthetic receive aperture imaging with phase correction for motion and for tissue ihomogeneities — part I: Basic principles,* IEEE Trans. Ultrason. Ferroelec. Freq. Contr., 39(4), 1992, 489–495.

[6] S. Holm, Focused multi-element synthetic aperture imaging. Department of Informatics, University of Oslo, 1995.

[7] I. Trots, A. Nowicki, M. Lewandowski, *Synthetic transmit aperture in ultrasound imaging,* Archives of Acoustics, 34 (4), 2009, 685 – 695.

[8] A. R. Selfridge, G. S. Kino, B. T. Khuri-Yakub, *A theory for the radiation pattern of a narrow-strip acoustic transducer*, Appl. Phys.Lett., 37 (1), 1980, 35-36.

[9] http://server.electro.dtu.dk/personal/jaj/field/

[10] K. Michishita, K. Sakagami, M. Morimotgo, U. P. Svensson, *Sound radiation from an unbaffled elastic plate strip of infinite length*, Applied Acoustics 61, 2000, 45-63.